Resilient Off-grid Microgrids: Capacity Planning and N-1 Security

Sreenath Chalil Madathil* *Member, IEEE*, Emre Yamangil†, Harsha Nagarajan†, Arthur Barnes†, Russell Bent†, Scott Backhaus†, Scott J. Mason*, Salman Mashayekh‡ *Member, IEEE,* Michael Stadler‡ *Member, IEEE*

***Abstract*—Over the past century the electric power industry has evolved to support the delivery of power over long distances with highly interconnected transmission systems. Despite this evolution, some remote communities are not connected to these systems. These communities rely on small, disconnected distribution systems, i.e., microgrids to deliver power. However, as microgrids often are not held to the same reliability standards as transmission grids, remote communities can be at risk for extended blackouts. To address this issue, we develop an optimization model and an algorithm for capacity planning and operations of microgrids that include N-1 security and other practical modeling features like AC power flow physics, component efficiencies and thermal limits. We demonstrate the computational effectiveness of our approach on two test systems; a modified version of the IEEE 13 node test feeder and a model of a distribution system in a remote community in Alaska.**

***Index Terms*—Off-grid microgrid, mathematical programming, security-constrained power flow, decomposition algorithm**

I. Introduction

ENERGY independence has been a common topic in the United States (US) since 1973 [1]. Energy independence is defined as the state in which national policy decisions on energy generation, transmission, and distribution are made without influence from external energy producing entities [2]. Energy independence is a difficult goal to achieve, especially for county governments and local communities in rural areas with limited or no connectivity to the bulk transmission system. For these communities, microgrids integrated with local energy sources and storage can help to reduce dependence on fossil fuels [3].

In addition to facilitating energy independence in rural communities, microgrids have the potential for improving resilience and reliability in the bulk transmission systems. During large-scale, extreme events, such as Superstorm Sandy [4], large parts of the bulk transmission system were de-energized, leaving many communities without power. Microgrids with distributed generation would allow these communities to supply power to their customers. Both of these situations present new challenges in reliability in the operation of distribution-scale systems.

In this work, we develop a mixed-integer, quadratically constrained, quadratic programming (MIQCQP) problem that minimizes capacity installation cost and operations cost of an off-grid (or disconnected) microgrid. Without connections to local utility grids, reliability is crucial for such disconnected microgrids. Thus, we introduce N-1 security constraints to our planning problem (Figure 1). The MIQCQP also models the linearized dist-flow (*LinDistFlow*) [5] ac physics of distribution systems over a full day (in 15 minute intervals) and includes capacity expansion options such as storage and energy sources. We also model the nonlinear efficiency curves associated with these devices using a piecewise linear approximation. We develop a scenario-based decomposition (SBD) algorithm to solve this problem and use both the IEEE 13 node test feeder and a model of a remote community in Alaska to test our approach. In short, the key contributions of this paper are:

- To the best of our knowledge, the first model of distribution system planning that simultaneously includes a nonlinear approximation of ac physics, time-extended operations, capacity expansion, N-1 reliability, and power device efficiencies.
- An algorithm that efficiently solves this problem.
- Demonstration on real system data and empirical validation of the results.

Literature review: The most similar work to this paper is the decision support tool DER-CAM that was developed by Lawrence Berkley National Lab (LBNL). DER-CAM is a decision support tool for decentralized energy systems that is used to plan, install, and operate various distributed energy resources (DER) like distribution generators for buildings and microgrids [6]. DER-CAM is used as a guide to determine technology installations, provide details about operational schedules at each time, and assess the market potential of various technologies for various communities. Baily *et al.* conducted the first study on modeling real-world installations of microgrids by applying the DER-CAM [7]. In many ways, our model is a direct extension of DER-CAM, with a number of key enhancements. In the earliest paper associated with

Manuscript received 11/02/2016; Corresponding author: Sreenath Chalil Madathil (email: schalil@g.clemson.edu). Authors are with *Department of Industrial Engineering, Clemson University, Clemson, SC 29634 USA, †Center for Nonlinear Studies, Los Alamos National Laboratory, Los Alamos, NM, USA, ‡Energy Storage and Distributed Resources Division, Lawrence Berkeley National Laboratory, CA, USA

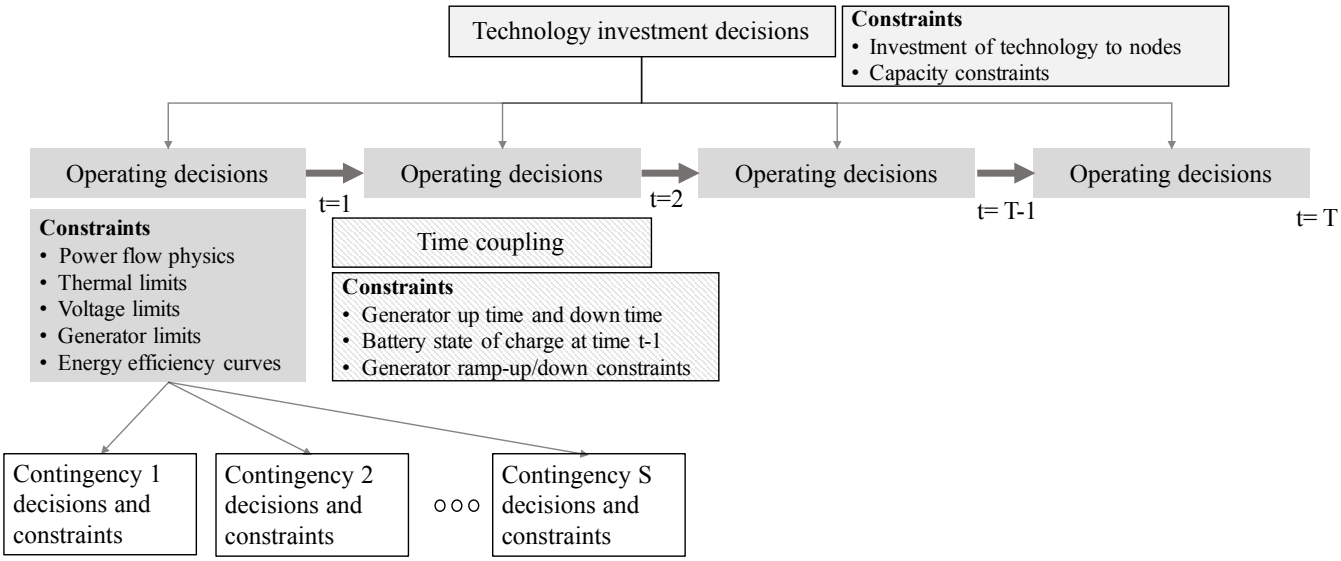

Figure 1. This flow chart describes the stages of the problem. At the top are the technology investment variables. The investments are applied at each operating time point (second level of the diagram). The operating decisions are connected via coupling constraints like ramping requirements. Each operating decision is further constrained by contingency requirements in the third stage (the figure only shows contingency constraints for $t = 1$.).

DER-CAM [8], the model focused on designing economical microgrids that satisfy customer demands and power flow physics. The model did not include security constraints, a significant source of computational complexity. In related work [9], authors extended the DER-CAM model and included decision variables associated with DER technology installation, DER capacity, operating status over time, and the cost of electricity. [10] later expanded the model to include an assessment of distribution network reliability. However, they did not include siting of resources or contingencies. Finally, Siddiqui *et al*. [11] discusses various advantages and applications of a localized network of DER.

A common thread in existing work has been a lack of contingency modeling. N-1 contingencies analysis has been studied in the context of transmission systems [17], [18], [19], [20], [21]. This is a rich area of study such as generalizations to unscheduled flows [22]. However, there is only limited work on N-1 (and other types of) security in distribution systems. Hayashi and Matsuki [23] discuss a tabu-search algorithm to determine optimal configuration of a distribution system with N-1 security. The model determines the status of switches, whether it is active or inactive, that connects distribution generators (DG) to the grid.

Concurrent work [24] in DER-CAM strongly motivates the need for N-1 security with a detailed case study. That paper includes much of the modeling detail included here and uses a linear approximation of the ac physics. Here, we address the scalability issues raised in [24], strengthen the approximation of ac physics with a convex quadratic formulation, and evaluate the quality of solutions obtained with the approximation.

Similar to N-1 security in distribution systems, there is limited work on models that include efficiencies of all components in the system. Bischi *et al*. [25] present a mixed integer linear program (MILP) model for planning the operation of combined cooling heating and power (CCHP) energy systems. They initially modeled the component efficiencies as non-linear constraints and then used a piecewise linearized approximation of the non-linear equations. Bahramirad *et al*. [26] develop a mathematical model to determine optimal sizing of an energy storage system and include constraints on the reliability of the system. They calculated the reliability index as the expected load curtailment in each reduced scenario and constraints are added to limit the loss of load expectation to certain threshold value.

Apart from developing mathematical models for designing and operating microgrids, there are several models that utilize the results of simulations. Hafez and Bhattacharya [27] develop a simulation model for the optimal design, planning, sizing, and operation of a hybrid renewable energy system (HRES). The authors use Homer® to select the capacity of generation and storage resources. More generally, Bahramara *et al*. [28] provide a list of problems that uses Homer software to solve design and operation of HRES. Bie *et al*. [29] use a non-sequential Monte Carlo simulation method to evaluate the reliability of distribution systems by considering multiple contingencies in the network. Table I lists the most related papers to our work and highlights key differences. Based on Table I, we believe this paper is the first to combine N-1 security with the design and operation of off-grid microgrids.

TABLE I. Models used in microgrid design

	Power Flow Physics	Technology Siting	Resource Capacity	Design Horizon	Demand Data	N-1 Security	Efficiencies	Batteries	Comments
[11]	NM	✓	✓	24 hours	hourly	×	×	×	
[12]	CM	✓	✓	24 hours	hourly	×	×	×	Simulation using Homer
[13]	NM	✓	✓	1 year	1 day / month	×	×	✓	
[14]	NM	×	✓	24 hours	hourly	×	×	✓	
[15]	NM	×	✓	24 hours	hourly	×	✓	✓	
[16]	NM	×	×	24 hours	hourly	✓	×	✓	
This Paper	*LinDistFlow*	✓	✓	24 hours	15 minutes	✓	✓	✓	

NM - Network flow Model CM - Capacity model

The rest of the paper is organized as follows: Section II introduces the mathematical formulation for the design and operation of off-grid microgrids with resource siting, power-flow physics, line limits, operational constraints, resource limits and storage efficiency. Section II also discusses the formulation of N-1 security constraints. Section III presents our algorithm for solving the model efficiently. Numerical results on two case studies are discussed in Section IV. Finally, Section V presents conclusions and future directions of research.

II. Mathematical Formulation

In this section we introduce the model for operating and planning microgrids for N-1 security. A power system is defined by a graph structure, where nodes correspond to buses and edges correspond to lines and transformers. Each bus may have energy resources that facilitate the production and transfer of power. Energy resources are sized in continuous or discrete capacity increments. For example, solar panels and storage resources, like batteries, are typically modeled as continuous capacity resources, whereas diesel and wind generators are modeled as discrete capacity resources. From an operational standpoint, resources are operated continuously (solar panels, hydro-electric generators, and wind turbines) or can be turned on or off at discrete time intervals (diesel generators). In short, most storage resources are modeled continuously and are classified as continuous operation resources. Generator resources are modeled continuously or discretely depending on their operation requirements. Each bus has a parametrized maximum number of continuous and discrete resources that may be installed. Each discrete resource is assigned to a specific slot (for contingency modeling) at a bus. Slots are used only for discrete resources to identify the number of discrete technology options that can be installed at a bus. We assume that generators that are at nodes with greater than one slot are installed in descending order of their maximum capacity. This assumption drastically increases the computational efficiency by avoiding a combinatorial explosion of possible installations at a node.

A. Model Parameters and Variables

Nomenclature

Sets

N	set of nodes (buses), indexed by i
$\mathcal{E}$	set of edges (lines and transformers), indexed by ij
$N^C \subseteq N$	set of nodes with continuous resources, indexed by i
$N^{CB} \subseteq N$	set of nodes with continuous resources with storage capabilities, indexed by i
$N^D \subseteq N$	set of nodes with discrete resources, indexed by i
$N_G(i)$	neighborhood of bus i, indexed by j
$K(i)$	number of slots at bus i, indexed by k_i
T	set of time periods, indexed by t
C	set of continuous resource options, indexed by c
$C^D \subseteq C$	set of continuous resource options with discrete operation, indexed by c
$C^C \subseteq C$	set of continuous resource options with continuous operation, indexed by c
$C^B \subseteq C^C$	set of continuous battery resource options, indexed by c
D	set of discrete resource options, indexed by d
$D^D \subseteq D$	set of discrete resource options with discrete operation, index by d
$D^C \subseteq D$	set of discrete resource options with continuous operation, indexed by d
$A = C \cup D$	set of all resource options, indexed by a
S	set of scenarios for N-1 security analysis, indexed by s

Parameters

FC_a	fixed cost for resource $a \in A$, (\$)
VC_a	variable cost for resource $a \in A$, (\$/MW)
$\mathrm{OC}_{a,0}$	fixed operational cost for resource $a \in A$, (\$)
$\mathrm{OC}_{a,1}$	linear operational cost for resource $a \in A$, (\$/MW)
$\mathrm{OC}_{a,2}$	quadratic operational cost for resource $a \in A$, (\$/(MW)^2)
UT_d , DT_d	minimum up-time and down-time for resource $d \in D$, (time-step)
RU_d , RD_d	ramp up and ramp down rate for resource $d \in D$, (MW/time-step)
$\tilde{\mathrm{T}}_{ij}$	apparent power thermal limit on line $ij \in \mathcal{E}$, (MVA)
$\mathrm{Pd}_i^t, \mathrm{Qd}_i^t$	Active and reactive power demand at bus $i \in N$ at time $t \in T$, (MW, MVAr)
$\overline{\mathrm{Pgd}}_d, \overline{\mathrm{Qgd}}_d$	maximum active and reactive power generated by a discrete resource $d \in D$ at time $t \in T$, (MW, MVAr)
$\underline{\mathrm{Pgd}}_d, \underline{\mathrm{Qgd}}_d$	minimum active and reactive power generated by a discrete resource $d \in D$ at time $t \in T$, (MW)
$\overline{\mathrm{Ssc}}_c$	maximum energy storage capacity of the battery, (MVA)
$\underline{\mathrm{V}}_i, \overline{\mathrm{V}}_i$	Squared voltage lower and upper bound at bus $i \in N$, $((kV)^2)$
M_c	maximum capacity for continuous resource, (MVA)
P	Number of pieces for piecewise linearization
L_a^p	Stand-by loss (y intercept) of a resource $a \in A$ for

each piecewise function $p \in \{1, .., P\}$, (MW)
η_a^p Marginal efficiency at $\pi_p^a\%$ of maximum rated power for each piece $p \in \{1, .., P\}$, (%)
$\mathrm{R}_{ij}, \mathrm{X}_{ij}$ Resistance and reactance of line $ij \in \mathcal{E}$, $(k\Omega)$
Δt time step, (hr)
C_{num} Maximum number of continuous resources at a bus

Binary decision variables: Discrete technology
$x_{i,d,k}^t$ active/inactive status for generator $d \in D$ at node $i \in N^D$ for slot $k \in K_i$ at time $t \in T$
$y_{i,d,k}^t$ start-up status for generator $d \in D$ at node $i \in N^D$ for slot $k \in K_i$ at time $t \in T$
$w_{i,d,k}^t$ shut-down status for generator $d \in D$ at node $i \in N^D$ for slot $k \in K_i$ at time $t \in T$
$\mathcal{B}\mathrm{gd}_{i,d,k}$ status indicator if discrete resource of type $d \in D$ is built at node $i \in N^D$ for slot $k \in K_i$

Binary decision variables: Continuous technology
$\mathcal{B}\mathrm{gc}_{i,c}$ status indicator if continuous resource of type $c \in C$ is built at node $i \in N^C$

Continuous decision variables: Discrete technology
$\mathrm{Pgd}_{i,d,k}^t$ ac active power generation during time $t \in T$ for slot $k \in K$ at node $i \in N$ using discrete resource $d \in D$, (MW)
$\mathrm{Qgd}_{i,d,k}^t$ ac reactive power generation during time $t \in T$ for slot $k \in K$ at node $i \in N$ using discrete resource $d \in D$, (MVAr)
$\mathrm{Pgd\_in}_{i,d,k}^t$ ac active power generation before losses during time $t \in T$ for slot $k \in K$ at node $i \in N$ using discrete resource $d \in D$, (MW)

Continuous decision variables: Continuous technology
$\mathrm{Pgc}_{i,c}^{\max}, \mathrm{Qgc}_{i,c}^{\max}$ maximum capacity of apparent power generation for continuous resource, $c \in C \setminus C^B$ for node $i \in N$, (MW, MVAr)
$\mathrm{Pgc}_{i,c}^t, \mathrm{Qgc}_{i,c}^t$ ac apparent power generation during time $t \in T$ at node $i \in N$ using continuous resource $c \in C$, (MW, MVAr)
$\mathrm{Pgc\_in}_{i,c}^t$ ac active power generation before losses during time $t \in T$ at node $i \in N$ using continuous resource $c \in C$, (MW)
$\mathrm{S}_{i,c}^{\max}$ maximum capacity of apparent power generation for continuous battery resource, $c \in C^B$ for node $i \in N$, (MVA)
$\mathrm{Ssc}_{i,b}^t$ Energy stored (state of charge) in the continuous resource battery $c \in C^B$ at time $t \in T$ at node $i \in N$, (MW-hr)

Continuous decision variables: Others
$\mathrm{Ndk}_{i,k}$ capacity of a slot at a node, $i \in N$ for slot $k \in K$, (MW)
$\mathrm{P}_{ij}^t, \mathrm{Q}_{ij}^t$ Active and reactive power flow though edge $ij \in \mathcal{E}$ at time $t \in T$, (MW, MVAr)
V_i^t Squared voltage at node $i \in N$ at time $t \in T$, $((kV)^2)$

B. Base Model

The objective function (1a) minimizes the total installation and operation cost of energy resources. The installation costs for continuous resources consist of a fixed cost and a sizing (variable) cost while the installation cost for discrete resources consist only of a fixed cost. These costs are equal to zero when a resource is already present. The operating costs of resources are modeled with quadratic functions of the form $CF = aP^2 + bP + c$ [15], where a, b and c are cost coefficients.

$$\min \sum_{i \in N^C} \Bigg(\sum_{c \in C} (\mathcal{B}\mathrm{gc}_{i,c})(\mathrm{FC}_c) + \sum_{c \in C \setminus C^B} (\mathrm{Pgc}_{i,c}^{\max})(\mathrm{VC}_c) + \sum_{c \in C^B} (\mathrm{S}_{i,c}^{\max})(\mathrm{VC}_c) \Bigg) + \sum_{i \in N^D} \sum_{d \in D} \sum_{k \in K_i} (\mathcal{B}\mathrm{gd}_{i,d,k})(\mathrm{FC}_d) + \sum_{t \in T} \sum_{i \in N^C} \sum_{c \in C \setminus C^B} \big((\mathrm{Pgc\_in}_{i,c}^t)^2 (\mathrm{OC}_{c,2}) + (\mathrm{Pgc\_in}_{i,c}^t)(\mathrm{OC}_{c,1}) + (\mathcal{B}\mathrm{gc}_{i,c})(\mathrm{OC}_{c,0}) \big) + \sum_{t \in T} \sum_{i \in N^D} \sum_{d \in D} \sum_{k \in K_i} \big((\mathrm{Pgd\_in}_{i,d,k}^t)^2 (\mathrm{OC}_{d,2}) + (\mathrm{Pgd\_in}_{i,d,k}^t)(\mathrm{OC}_{d,1}) + (x_{i,d,k}^t)(\mathrm{OC}_{d,0}) \big) \tag{1a}$$

Power Flows: Nodal flow balance is enforced by constraints (2a) and (2b).

Constraints (2c) ensure that line thermal limits are enforced during operations. The linearized version of ac power flow physics is modeled in constraints (2d). For computational tractability, we use the single-phase, *LinDistFlow* equations of [5], [30] (the model is convex-quadratic when *LinDistFlow* constraints are added). We show in our empirical results that the approximations are reasonable to use here.

Finally, voltage bounds are enforced using constraints (2e).

$$\sum_{c \in C} (\mathrm{Pgc}_{i,c}^t) + \sum_{d \in D} \sum_{k \in K_i} (\mathrm{Pgd}_{i,d,k}^t) - (\mathrm{Pd}_i^t) = \sum_{\substack{ij \in \mathcal{E} \\ j \in N_G(i)}} \mathrm{P}_{ij}^t \quad \forall\, i \in N, t \in T \tag{2a}$$

$$\sum_{c \in C} (\mathrm{Qgc}_{i,c}^t) + \sum_{d \in D} \sum_{k \in K_i} (\mathrm{Qgd}_{i,d,k}^t) - (\mathrm{Qd}_i^t) = \sum_{\substack{ij \in \mathcal{E} \\ j \in N_G(i)}} \mathrm{Q}_{ij}^t \quad \forall\, i \in N, t \in T \tag{2b}$$

$$(\mathrm{P}_{ij}^t)^2 + (\mathrm{Q}_{ij}^t)^2 \leq (\tilde{\mathrm{T}}_{ij})^2 \quad \forall\, ij \in \mathcal{E}, t \in T \tag{2c}$$

$$V_j^t = V_i^t - 2(\mathrm{R}_{ij}\mathrm{P}_{ij}^t + \mathrm{X}_{ij}\mathrm{Q}_{ij}^t) \quad \forall\, ij \in \mathcal{E}, t \in T \tag{2d}$$

$$(\underline{\mathrm{V}_i}) \leq V_i^t \leq (\overline{\mathrm{V}_i}) \quad \forall\, i \in N, t \in T \tag{2e}$$

Resource Limits: Constraints (3a) through (3c) ensure that the output of continuous resources is limited by the installed capacity. Constraint (3d) limits the number of continuous technologies installed per bus. Similarly, constraints (3e) and (3f) bound the output of discrete resources with continuous operation.

$$\text{Pgc}_{i,c}^t \le \text{Pgc}_{i,c}^{\max} \le \mathcal{B}\text{gc}_{i,c} M_c \quad \forall\, i \in N^C, c \in C \setminus C^B, t \in T \tag{3a}$$

$$\text{Qgc}_{i,c}^t \le \text{Qgc}_{i,c}^{\max} \le \mathcal{B}\text{gc}_{i,c} M_c \quad \forall\, i \in N^C, c \in C, t \in T \tag{3b}$$

$$\text{S}_{i,c}^{\max} \le \mathcal{B}\text{gc}_{i,c} M_c \;\; \forall\, i \in N^{CB}, c \in C^B \tag{3c}$$

$$\sum_{c \in C} \mathcal{B}\text{gc}_{i,c} \le C_{\text{num}} \;\forall\, i \in N^C \tag{3d}$$

$$\underline{\text{Pgd}}_d \mathcal{B}\text{gd}_{i,d,k} \le \text{Pgd\_in}_{i,d,k}^t \le \overline{\text{Pgd}}_d \mathcal{B}\text{gd}_{i,d,k} \quad \forall\, i \in N^D, d \in D^C, k \in K_i, t \in T \tag{3e}$$

$$\underline{\text{Qgd}}_d \mathcal{B}\text{gd}_{i,d,k} \le \text{Qgd}_{i,d,k}^t \le \overline{\text{Qgd}}_d \mathcal{B}\text{gd}_{i,d,k} \quad \forall\, i \in N^D, d \in D^C, k \in K_i, t \in T \tag{3f}$$

Resource Slots: Constraints (4a) are assignment constraints that ensure each node's slot contains at most one discrete resource.

Constraints (4b) and (4c) are symmetry-breaking constraints that order slot assignments by resource capacity.

$$\sum_{d \in D} \mathcal{B}\text{gd}_{i,d,k} \le 1 \;\forall\, i \in N^D, k \in K_i \tag{4a}$$

$$\text{Ndk}_{i,k} = \sum_{d \in D} \overline{\text{Pgd}}_d \mathcal{B}\text{gd}_{i,d,k} \;\forall\, i \in N^D, k \in K_i \tag{4b}$$

$$\text{Ndk}_{i,k} \ge \text{Ndk}_{i,k+1} \;\forall\, i \in N^D, k \in K_i, k < |K_i| \tag{4c}$$

Discrete Operation of Resources: Constraints (5a) and (5b) link resource output to the active or inactive status of the resource.

The resource status is linked to the installation choice through constraints (5c).

Constraints (5d) then ensure that activated discrete resources are active for a minimum time period. Similarly, constraints (5e) ensure deactivated resources are inactive for a minimum time period. This is a pessimistic model of generator operations that does not allow the boundary conditions at $t = 0$ or $t = T$ to relax the requirements on UT or DT. Without loss of generality, UT and DT could be adjusted at the boundaries to support more optimistic models of generator operations at the boundaries of the model.

Constraints (5f) and (5g) link the resource indicator variables x, y, and w together. Constraints (5h) and (5i) enforce resource ramping rates between time periods.

Finally, constraints (5a) through (5i) are applied for all $i \in N^D, d \in D^D, k \in K_i, t \in T$

$$\underline{\text{Pgd}}_d x_{i,d,k}^t \le \text{Pgd\_in}_{i,d,k}^t \le \overline{\text{Pgd}}_d x_{i,d,k}^t \tag{5a}$$

$$\underline{\text{Qgd}}_d x_{i,d,k}^t \le \text{Qgd}_{i,d,k}^t \le \overline{\text{Qgd}}_d x_{i,d,k}^t \tag{5b}$$

$$x_{i,d,k}^t \le \mathcal{B}\text{gd}_{i,d,k} \tag{5c}$$

$$\sum_{j=t}^{t+(\min(\text{UT}_d, T-t))} x_{i,d,k}^j \ge (\text{UT}_d) y_{i,d,k}^t \tag{5d}$$

$$\sum_{j=t}^{t+(\min(\text{DT}_d, T-t))} x_{i,d,k}^j \le (\text{DT}_d)(1 - w_{i,d,k}^t) \tag{5e}$$

$$x_{i,d,k}^t = x_{i,d,k}^{t-1} + y_{i,d,k}^t - w_{i,d,k}^t \tag{5f}$$

$$y_{i,d,k}^t + w_{i,d,k}^t \le 1 \tag{5g}$$

$$\text{RD}_d \ge \text{Pgd}_{i,d,k}^{t-1} - \text{Pgd}_{i,d,k}^t - \overline{\text{Pgd}}_d w_{i,d,k}^t \tag{5h}$$

$$\text{RU}_d \ge \text{Pgd}_{i,d,k}^t - \text{Pgd}_{i,d,k}^{t-1} - \overline{\text{Pgd}}_d y_{i,d,k}^t \tag{5i}$$

Storage: Apparent power limits on charging and discharging are stated in constraints (6a). Constraints (6b) link the state of charge to energy extraction, while constraints (6c) bounds storage charging and discharging with maximum charging and discharging capacity. The charging and discharging constraints are modelled using the constraints presented by Iordanis *et al.* [31] Constraints (6a) through (6c) are applied to all $i \in N^{CB}, c \in C^B, t \in T$

$$(\text{Pgc}_{i,c}^t)^2 + (\text{Qgc}_{i,c}^t)^2 \le (\text{S}_{i,c}^{\max})^2 \tag{6a}$$

$$\text{Ssc}_{i,c}^t = \text{Ssc}_{i,c}^{t-1} - \text{Pgc\_in}_{i,c}^t \Delta t \tag{6b}$$

$$0 \le \text{Ssc}_{i,c}^t \le \overline{Ssc_c} \tag{6c}$$

Efficiencies: Fig. 2 depicts an example of a piecewise linear convex relaxation of the relationship between power generated in kW and output power in kW. The power curves, efficiencies, and specifications of various resources are found in [32], [33], [34], [35] and [36]. We parametrized these piecewise linear relaxed efficiency curve using these specification sheets, however, these choices are provided as user input. More specifically, the input-output relationship is

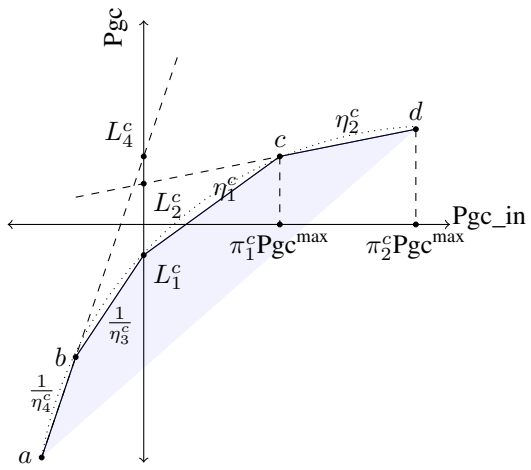

Figure 2. An illustrative example of a piecewise linear efficiency curve

a set of linear functions defined by constraints (7a) through (7c) that apply efficiency curves to continuous as well as discrete resources at all nodes $i \in N$, time periods $t \in T$ and slots $k \in K_i$ for each linearization of piecewise function $p \in \{1, .., P\}$. In our models we have used P = 4.

$$\text{Pgc}_{i,c}^t \le \eta_c^p \text{Pgc\_in}_{i,c}^t + \mathcal{B}\text{gc}_{i,c} L_c^p \quad \forall\, c \in C \tag{7a}$$

$$\text{Pgd}_{i,d,k}^t \le \eta_d^p \text{Pgd\_in}_{i,d,k}^t + x_{i,d,k}^t L_d^p \quad \forall\, d \in D^C \tag{7b}$$

$$\text{Pgd}_{i,d,k}^t \le \eta_d^p \text{Pgd\_in}_{i,d,k}^t + \mathcal{B}\text{gd}_{i,d,k} L_d^p \quad \forall\, d \in D^D \tag{7c}$$

C. N-1 Security Constraints

In this section, we generalize our model to include security constraints. Without loss of generality, we assume the contingencies are N-1 line and generator contingencies[1]. Once again, without loss of generality, in this study we only include continuous generators and the largest-capacity discrete generators in the security analysis set.

Objective Function: In objective function (8a), we add variables that account for the amount of power that is not served during each of the contingencies to the objective function defined in (1a), where μ is a penalty variable that penalizes power-not-served (PNS). Decision variables $Pns^s_{i,t}$, and $Qns^s_{i,t}$ are unrestricted shedding variables that measure the active and reactive power that are not served. Generally, $Pns = 0$ is the goal for all contingencies.

$$\min\ (1a)\ + \mu\Bigg(\sum_{i\in N}\sum_{t\in T}\sum_{s\in S}(|Pns^s_{i,t}| + |Qns^s_{i,t}|)\Bigg) \tag{8a}$$

Contingency variables for power flow variables are indexed by $s \in S$, such as $\mathrm{Pgc}^{t,s}_{i,c}$, $\mathrm{Pgd}^{t,s}_{i,d,k}$, $\mathrm{P}^{t,s}_{ij}$, $\mathrm{Qgc}^{t,s}_{i,c}$, $\mathrm{Qgd}^{t,s}_{i,d,k}$, $\mathrm{Q}^{t,s}_{ij}$, and $\mathrm{V}^{t,s}_{i}$. For N-1 security analysis, we add new variables to the power flow constraints defined in (2a) and (2b) of the base model. The power flow equations include PNS for active ($Pns^s_{i,t}$) and reactive power ($Qns^s_{i,t}$) load shedding.

$$\begin{aligned} &Pns^s_{i,t} + \sum_{c\in C}(\mathrm{Pgc}^{t,s}_{i,c}) + \sum_{d\in D}\sum_{k\in K_i}(\mathrm{Pgd}^{t,s}_{i,d,k}) - (\mathrm{Pd}^t_i) \\ &= \sum_{\substack{ij\in\mathcal{E}\\ j\in N_G(i)}} \mathrm{P}^{t,s}_{ij} \quad \forall\ i\in N, t\in T, s\in S \end{aligned} \tag{9a}$$

$$\begin{aligned} &Qns^s_{i,t} + \sum_{c\in C}(\mathrm{Qgc}^{t,s}_{i,c}) + \sum_{d\in D}\sum_{k\in K_i}(\mathrm{Qgd}^{t,s}_{i,d,k}) - (\mathrm{Qd}^t_i) \\ &= \sum_{\substack{ij\in\mathcal{E}\\ j\in N_G(i)}} \mathrm{Q}^{t,s}_{ij} \quad \forall\ i\in N, t\in T, s\in S \end{aligned} \tag{9b}$$

Discrete resources contingency: Security analysis for the discrete resources is modeled using constraints (10a). The indexes in constraints (10a) i, d, k, and t represent the contingent scenario $s \in S$ which includes generator d installed at slot $k = 1$ of node i that faults during time t. The discrete resources and ramp factors (Δd_d) are tied to the resources' active/inactive variable $x^t_{i,d,k}$, whereas discrete resources with continuous operation are tied to the installation variable, $\mathcal{B}\mathrm{gd}_{i,d,k}$. Constraints (10b) through (10e) are applied for all non-contingent discrete resources that belongs to $i \in N, k \in K_i, t \in T$.

$$\mathrm{Pgd}^{t,s}_{i,d,k} = 0, \qquad \mathrm{Qgd}^{t,s}_{i,d,k} = 0\ \forall\ d\in D \tag{10a}$$

$$\begin{aligned} &\mathrm{Pgd}^t_{i,d,k} - \Delta d_d x^t_{i,d,k} \le \mathrm{Pgd}^{t,s}_{i,d,k} \le \\ &\qquad \mathrm{Pgd}^t_{i,d,k} + \Delta d_d x^t_{i,d,k}\ \forall\ d\in D^D \end{aligned} \tag{10b}$$

$$\begin{aligned} &\mathrm{Qgd}^t_{i,d,k} - \Delta d_d x^t_{i,d,k} \le \mathrm{Qgd}^{t,s}_{i,d,k} \le \\ &\qquad \mathrm{Qgd}^t_{i,d,k} + \Delta d_d x^t_{i,d,k}\ \forall\ d\in D^D \end{aligned} \tag{10c}$$

$$\begin{aligned} &\mathrm{Pgd}^t_{i,d,k} - \Delta d_d \mathcal{B}\mathrm{gd}_{i,d,k} \le \mathrm{Pgd}^{t,s}_{i,d,k} \le \\ &\qquad \mathrm{Pgd}^t_{i,d,k} + \Delta d_d \mathcal{B}\mathrm{gd}_{i,d,k}\ \forall\ d\in D^C \end{aligned} \tag{10d}$$

$$\begin{aligned} &\mathrm{Qgd}^t_{i,d,k} - \Delta d_d \mathcal{B}\mathrm{gd}_{i,d,k} \le \mathrm{Qgd}^{t,s}_{i,d,k} \le \\ &\qquad \mathrm{Qgd}^t_{i,d,k} + \Delta d_d \mathcal{B}\mathrm{gd}_{i,d,k}\ \forall\ d\in D^C \end{aligned} \tag{10e}$$

When there is a contingency for a discrete resource, all continuous resources can adjust their power generation within certain limits defined by the ramp factor for those resources. Constraints (11a) and (11b) ensure that the ramping for continuous resources is within ramp limits (Δc_c) and is applied for all $i \in N, c \in C, t \in T, s \in S$.

$$\mathrm{Pgc}^t_{i,c} - \Delta c_c \mathcal{B}\mathrm{gc}_{i,c} \le \mathrm{Pgc}^{t,s}_{i,c} \le \mathrm{Pgc}^t_{i,c} + \Delta c_c \mathcal{B}\mathrm{gc}_{i,c} \tag{11a}$$

$$\mathrm{Qgc}^t_{i,c} - \Delta c_c \mathcal{B}\mathrm{gc}_{i,c} \le \mathrm{Qgc}^{t,s}_{i,c} \le \mathrm{Qgc}^t_{i,c} + \Delta c_c \mathcal{B}\mathrm{gc}_{i,c} \tag{11b}$$

Continuous resources contingency: Similar to discrete resource contingencies, continuous resource contingencies are modeled using constraints (12a). The indexes in constraints (12a) i, c, and t correspond to the contingent scenario s and generator c at node i that is faulted during time period t. Constraint (12b) sets the upper limit for the power generation by the continuous resource during contingency s and is applied for all $i \in N, t \in T, c \in C, s \in S$.

$$\mathrm{Pgc}^{t,s}_{i,c} = 0, \qquad \mathrm{Qgc}^{t,s}_{i,c} = 0 \tag{12a}$$

$$\mathrm{Pgc}^{t,s}_{i,c} \le \mathrm{Pgc}^{\max}_{i,c}, \quad \mathrm{Qgc}^{t,s}_{i,c} \le \mathrm{Qgc}^{\max}_{i,c} \tag{12b}$$

Finally, the thermal limit for security analysis is enforced using constraint (13a) and *LinDistFlow* is enforced by constraints (13b). The voltage limits are constrained by the constraints (13c). The constraints (13a) through (13c) are applied $\forall\ (i,j) \in N, ij \in \mathcal{E}, t \in T, s \in S$.

$$(\mathrm{P}^{t,s}_{ij})^2 + (\mathrm{Q}^{t,s}_{ij})^2 \le (\tilde{\mathrm{T}}_{ij})^2 \tag{13a}$$

$$\mathrm{V}^{t,s}_j = \mathrm{V}^{t,s}_i - 2(\mathrm{R}_{ij}\mathrm{P}^{t,s}_{ij} + \mathrm{X}_{ij}\mathrm{Q}^{t,s}_{ij}) \tag{13b}$$

$$\underline{\mathrm{V}_i} \le \mathrm{V}^{t,s}_i \le \overline{\mathrm{V}_i} \tag{13c}$$

III. Algorithms

A. Base algorithm

The first algorithm solves the whole model using a commercially available solver, Gurobi 6.5.0.

[1]The formulation can include a subset of N-1 contingencies or include sets of N-K contingencies

B. Scenario-based decomposition algorithm

We adopt a scenario-based decomposition (SBD) methodology whereby "scenarios" are added to the model one by one based on certain conditions. A scenario and contingency are used synonymously in our description of the SBD algorithm. Unrestricted shedding variables for the N-1 model, ($Pns^s_{i,t}$) and ($Qns^s_{i,t}$), identify the scenarios that cause infeasibility. The values of these variables are used to decide which scenario should be added to the model. The pseudo-code for the SBD algorithm is explained in Algorithm 1.

In the SBD algorithm, M denotes the mathematical model that is to be solved. Initially, M is the base model without N-1 security constraints, (Here, M consists of constraints (2a) through (7b)). A sub-problem ($SP1$) is defined for each of the contingent scenarios, as the model which includes objective function defined in (8a), without (1a), all constraints for an N-1 security analysis, and values of the variables from base model that are realized after solving the model M. Here, the objective function for $SP1$ minimizes $\sum_{i\in N}\sum_{t\in T}\sum_{s\in S}(|Pns^s_{i,t}| + |Qns^s_{i,t}|)$ and includes constraints (9a) through (13c). The objective function for sub-problem ($SP1$) for each of the contingencies s is stored in a vector $S_{obj}(s)$. The value of $S_{obj}(s) = \sum_{i\in N}\sum_{t\in T}(|Pns^s_{i,t}| + |Qns^s_{i,t}|) \quad \forall\ s \in S$. SBD is an exact algorithm whenever the sub-problems are feasibility problems. Here, the exactness criteria is met when $\max(S_{obj}) = 0$ in the optimal solution, i.e. the sub-problems reduce to feasibility problems.

Algorithm 1: Scenario-based decomposition

```
Define M as base model without the N-1 constraints ;
Define S_obj as the vector of size S ;
Create scenario set S, indexed by s, with all scenarios ;
while max(S_obj) > 0 or S = ∅ do
    Solve the model, M ;
    Get the values of base model decision variables, x̄ ;
    for s ∈ S do
        Solve sub-problem SP1 for scenario s using x̄;
        Update S_obj(s);
    end
    Set candidate scenario, s_c = index of max(S_obj);
    Add N-1 constraints for scenario s_c to model M;
    Update scenario set S = S \ s_c;
    Set S_obj(s_c) = 0;
end
```

IV. Numerical Results

We used Clemson University's high performance computing resource, the Palmetto Cluster, which has Intel® Xenon® CPU X7542, 24 core processors @ 2.67 GHz and 172 GB RAM. The optimization model and algorithms were implemented using JuMP [37] and Gurobi 6.5.0.

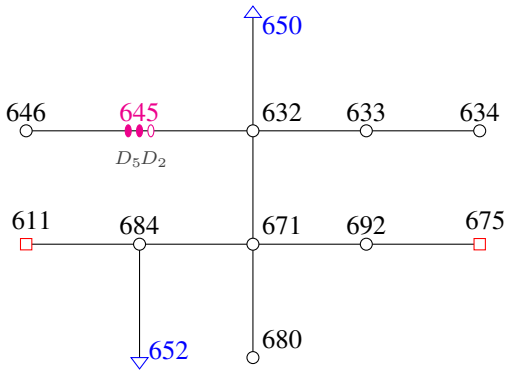

Figure 3. IEEE 13 node radial distribution test feeder

A. Case Study - IEEE 13

Our first case study uses the IEEE 13 node radial distribution test feeder [38], modified to use a positive-sequence representation (we use the constraint limits of [38]). This is illustrated in Fig. 3. In Fig. 3, red squares are nodes that have the ability to install continuous resources. Similarly, the blue triangular nodes can install discrete resources, while elliptical nodes (node 645) can accommodate both continuous and discrete resources. Demand data is for every 15 minutes (Δt=0.25 hours).

Demand data for this system is based on a New Mexico distribution utility. The characteristics of the technology options available are provided in Table II. We assume an efficiency of 95% for dispatched power $\leq 0.5 \times P_{rated}$ and 90% for dispatched power $> 0.5 \times P_{rated}$. We assume standby losses are 0.3 KW. The ramp-up and ramp-down rates are 200 KW per time-step.

TABLE II. Characteristics of technology options

Tech Type	Fixed Cost ($)	Variable Cost ($/KW)	Operational Cost aP^2+bP+c ($)	Rated Power (Max, Min) (KW)
C1	100	300	$10P^2+5P+2$	(100 , 0)
C2	200	250	$20P^2+10P+4$	(100 , 0)
C3	250	200	$30P^2+15P+8$	(100 , 0)
C4	300	150	$40P^2+20P+10$	(100 , 0)
C5	350	100	$50P^2+25P+5$	(100 , 0)
D1	200	0	$50P^2+25P+6$	(250 , −250)
D2	100	0	$40P^2+20P+5$	(275 , −250)
D3	250	0	$30P^2+15P+4$	(300 , −250)
D4	300	0	$20P^2+10P+3$	(225 , −250)
D5	350	0	$10P^2+5P+2$	(200 , −250)

Base Algorithm The solution times for design horizons of 5, 10, 15, 20, 50 and 96 time periods for the base algorithm are shown in Fig. 4. The 96 period (24 hours) design horizon problem took 1.5 hours to complete on the Palmetto cluster.
SBD In comparison with the base algorithm, SBD is able to solve the 96 period problem in roughly 18 minutes (Fig. 4), a factor of 5× speedup. For this case study, the SBD

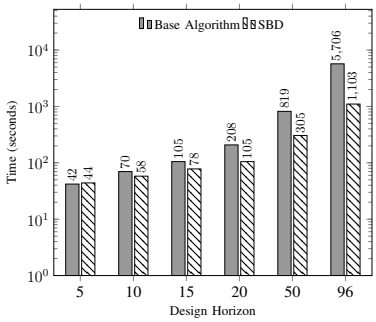

Figure 4. Results for the base algorithm and SBD

approach is more efficient than solving the entire problem using commercial solvers.

In this test case, devices D2 and D5 were installed at node 645. D5 is used more often than D2, due to its lower operational cost. The relative cost of N-1 security is provided in Fig. 5. Most of the difference in cost is due to dispatching D2 at higher levels to ensure N-1 feasibility.

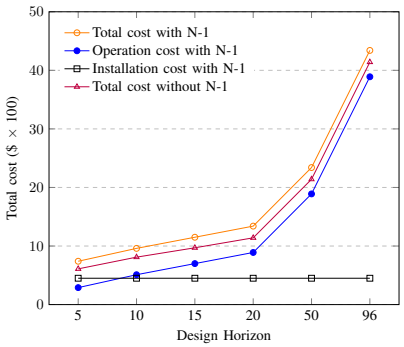

Figure 5. Total cost for each time period

B. Case Study - Alaskan Microgrid

We next present results based on the distribution circuits of a remote community in Alaska which was developed in [24]. There are 19 nodes in the network, whose schematic diagram is shown in Fig. 6. Node 1 has four generators and Node 3 has a wind generation unit. We ran the model with options to install generators at nodes 6, 8, 10, 14, and 18. These are nodes with critical loads including a hospital, airport, correctional center, gas station, and high school).

The characteristics of the technology options are provided in Table III. We used the same efficiencies as in the IEEE case. The ramp-up and ramp-down rates were set to 190 KW for D1 and 500 KW for the rest. Details of the full model are available upon request.

We ran the model for 5, 10, 15, 20, 30, 50, and 96 period design horizons with the base model and the SBD algorithm. The solution times for various design horizons are shown in Fig. 7. Interestingly, the base algorithm slightly outperforms

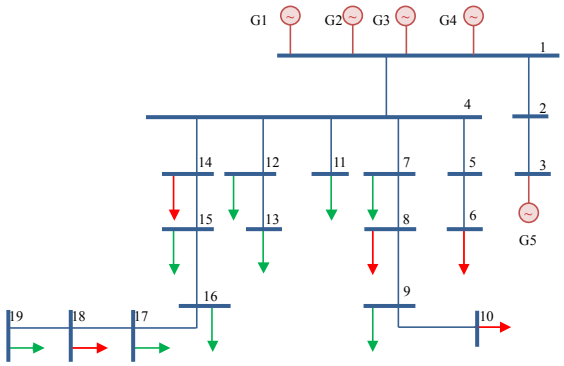

Figure 6. Schematic diagram of a remote community in Alaska

TABLE III. Characteristics of technology options for Alaskan microgrid

Tech Type	Fixed Cost ($)	Variable Cost ($/KW)	Operational Cost $aP2+bP+c$ ($)	Rated Power (Max, Min) (KW)
D1	200	0	$50P^2+25P+6$	(200 , 0)
D2,D3,D4,D5	500	0	$60P^2+20P+5$	(1500 , 0)

the SBD algorithm. In this case, none of the contingencies dominate the other, so all contingencies must be added (see Table IV). In this worst case for SBD, SBD becomes the base algorithm with extra computational overhead. However, this overhead was relatively small, suggesting that the potential benefits of SBD outweigh the risk of this behavior. An interesting area of future work considers enhancements to SBD to avoid this situation.

TABLE IV. Number of scenarios added by SBD

Case Study	Base Algorithm	SBD
IEEE 13	18	3
Alaskan Microgrid	7	7

Once again, the dispatch was adjusted to satisfy contingency constraints. The new dispatch reduces the power output from the generators installed at node 8 and 14 and increases the dispatch from all other generators. The overall increase in cost for this increased dispatch due to contingencies is $195k. This confirms the importance of including N-1 security as discussed in [24].

C. Sensitivity Analysis

It is important to understand the impact of including N-1 security constraints and component efficiencies (as compared to the prior models of Table I). Table V shows the impacts of introducing these modeling details to the IEEE 13 bus model. As expected, the computation time increases dramatically when N-1 security constraints are included in the model. Moreover, both efficiencies and N-1 can considerably alter the solutions themselves. For example, when efficiencies are

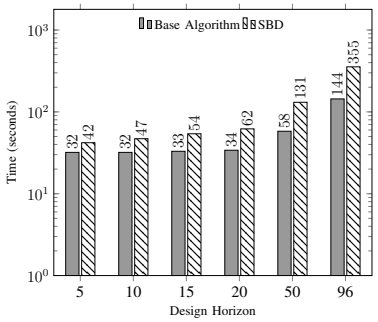

Figure 7. Solution time for Alaskan microgrid model using SBD

not modeled the total cost is reduced because generation is not required to cover the losses associated with storage. In short, there are three key observations contained in Table V. First, the sensitivity of the design choices are tied to whether or not N-1 contingencies are included in the model. Including these constraints forces the inclusion of additional resources. This result is common to both our model and prior work that has included N-1 constraints. Second, the inclusion of efficiencies significantly alters the operating cost (as much as 25%). Third, we note that the solutions are insensitive to the network flow, indicating, at least on this problem, that voltages are not an issue during the contingencies. We conjecture that a careful consideration of the voltage profiles during contingencies will provide insight on the importance of including these constraints on other problems. Finally, it is important to note that we have also indicated models described by prior literature in the last column of the table.

We also performed a sensitivity analysis on the various combinations of technology resources that are available for investment. Table VI considers solutions where discrete technology resources are available, continuous technology resources are available, and both are available. Interestingly, rows 1 and 3 have the same objective function and the same solution. Given the assumptions on the relative costs of the different resources, the discrete technologies are more desirable. When only continuous resources are allowed, the solution cost is considerably higher.

D. Feasible Solution Recovery

It is also important to validate the solutions obtained using the approximate *LinDistFlow* equations. Here, we used the *DistFlow* equations from Baran and Wu [30] for validation. The installation choices and commitment choices are fixed by the *LinDistFlow* solution. Knitro is used to find a locally optimal dispatch solution based on *DistFlow*. A feasible solution was always found and a comparison of the objective values is shown in Table VII. Generally speaking, the solutions found using *LinDistFlow* are a good approximation of what is necessary when modeling the full physics of the system.

V. Conclusions

In this paper, we develop a mathematical formulation for planning and operation of remote off-grid microgrids with N-1 security constraints and component efficiencies. We show that a scenario-based decomposition algorithm using a *LinDistFlow* approximation can effectively solve these problems based on results for a modified IEEE 13 bus and the Alaskan distribution feeder. The effectiveness of the approximation is validated with the full nonlinear ac physics. There remain a number of interesting future directions for this research. First, we need to scale this approach to model multiple days of potential demands corresponding to different usage requirements. Second, we have assumed a purely deterministic model of generation and future work will need to incorporate stochastic renewable resources (wind, solar), and the unscheduled flows associated with them [22]. Here, the probabilistic chance constraints of [39] are an attractive option. Third, resiliency criteria is also an important criteria to consider in the future. One possibility is to include criteria with constraints and additional planning scenarios as discussed in [40]. Finally, we also need to include topology design choices into the model to better reflect planning choices faced by microgrid designers.

Acknowledgements This work is partially funded by the Office of Electricity Delivery and Energy Reliability, Distributed Energy Program of the U.S. Department of Energy under Contract No. DE-AC02-05CH11231 and Work Order M615000466. We also want to thank Dan Ton from the Office of Electricity Delivery and Energy Reliability for supporting our work. Clemson University is acknowledged for generous allotment of compute time on Palmetto cluster. The Center for Nonlinear Studies at LANL also supported this work.

References

[1] D. Yergin, "Congratulations, america. you're (almost) energy independent," November 2013. [Online]. Available: http://goo.gl/o6QYPf

[2] D. L. Greene, "Measuring energy security: Can the united states achieve oil independence?" Energy policy, vol. 38, no. 4, pp. 1614–1621, 2010.

[3] M. Sciulli, "Remote off-grid microgrid design support tool research call," http://energy.gov/oe/articles/oe-announces-awardees-under-remote-grid-microgrid-design-support-tool-research-call, September 2015.

[4] M. Kunz, B. Mühr, T. Kunz-Plapp, J. Daniell, B. Khazai, F. Wenzel, M. Vannieuwenhuyse, T. Comes, F. Elmer, K. Schröter et al., "Investigation of superstorm sandy 2012 in a multi-disciplinary approach," Natural Hazards and Earth System Sciences, vol. 13, no. 10, pp. 2579–2598, 2013.

[5] L. Gan, N. Li, U. Topcu, and S. H. Low, "Exact convex relaxation of optimal power flow in radial networks," Automatic Control, IEEE Transactions on, vol. 60, no. 1, pp. 72–87, 2015.

[6] G. Cardoso, N. DeForest, L. Le Gall, C. Gehbauer, M. Hartner, S. Mashayekh, C. Milan, T. Schittekatte, M. Stadler, D. Steen, and J. Tjaeder, "DER-CAM user manual full DER web optimization service," Lawrence Berkeley National Laboratory (LBNL), 1 Cyclotron Rd, Berkeley, CA 94720, Tech. Rep., 2015. [Online]. Available: https://building-microgrid.lbl.gov/sites/all/files/DER-CAM%2B%20full%20manual.pdf

TABLE V. Sensitivity Analysis

S.No	N-1	Efficiency	Power flow Model	Run time Seconds	Objective cost ($)	Min. Voltage (kV)	Max. Voltage (kV)	Solution	References
1	×	✓	*LinDistFlow*	57	4137.51	3.952	3.954	D5 at Node 652	
2	×	✓	Network Model	29	4137.51	3.952	3.952	D5 at Node 650	[15]
3	×	×	*LinDistFlow*	503	3385.23	4.16	4.37	D5 at Node 650	
4	×	×	Network Model	424	3385.23	3.952	3.952	D5 at Node 645	[11], [13], [14]
5	✓	✓	*LinDistFlow*	5705	4337.51	3.952	3.954	D5 and D2 at Node 645	This paper
6	✓	✓	Network Model	1678	4337.51	3.952	3.952	D5 and D2 at Node 645	
7	✓	×	*LinDistFlow*	12143	3617.23	4.17	4.14	D5 and D2 at Node 645	
8	✓	×	Network Model	13467	3617.23	3.952	3.952	D5 and D2 at Node 645	[16]

TABLE VI. Sensitivity analysis with resource options

S.No	Continuous	Discrete	Objective function ($)	Run time (Sec.)
1	✓	✓	4337.5	5706
2	✓	×	12386.0	1042
3	×	✓	4337.5	59

TABLE VII. Gap for objective functions

Case Study	*LinDistFlow* ($)	*DistFlow* ($)	Gap (%)
IEEE 13	4337.51	4337.99	0.011
Alaskan Microgrid	66940641.76	68650106.97	2.490

[7] O. Bailey, C. Creighton, R. Firestone, C. Marnay, and M. Stadler, "Distributed energy resources in practice: A case study analysis and validation of LBNL's customer adoption model," Lawrence Berkeley National Laboratory, 2003.

[8] C. Marnay, R. Blanco, K. S. Hamachi, C. P. Kawaan, J. G. Osborn, and F. J. Rubio, "Integrated assessment of dispersed energy resources deployment," Lawrence Berkeley National Lab, 2000.

[9] F. J. Rubio, A. S. Siddiqui, C. Marnay, and K. S. Hamachi, "CERTS customer adoption model," Lawrence Berkeley National Lab, 2000.

[10] C. Marnay, J. S. Chard, K. S. Hamachi, T. Lipman, M. M. Moezzi, B. Ouaglal, and A. S. Siddiqui, "Modeling of customer adoption of distributed energy resources," Lawrence Berkeley National Lab, 2001.

[11] A. S. Siddiqui, C. Marnay, J. L. Edwards, R. Firestone, S. Ghosh, and M. Stadler, "Effects of carbon tax on microgrid combined heat and power adoption," Journal of Energy Engineering, 2005.

[12] S. Mizani and A. Yazdani, "Design and operation of a remote microgrid," in Industrial Electronics, 2009. IECON'09. 35th Annual Conf. of IEEE. IEEE, 2009, pp. 4299–4304.

[13] A. Saif, K. G. Elrab, H. Zeineldin, S. Kennedy, and J. Kirtley, "Multi-objective capacity planning of a pv-wind-diesel-battery hybrid power system," in Energy Conf. and Exhibition (EnergyCon), 2010 IEEE International. IEEE, 2010, pp. 217–222.

[14] E. Mashhour and S. Moghaddas-Tafreshi, "Integration of distributed energy resources into low voltage grid: A market-based multiperiod optimization model," Electric Power Systems Research, vol. 80, no. 4, pp. 473–480, 2010.

[15] A. Parisio and L. Glielmo, "A mixed integer linear formulation for microgrid economic scheduling," in Smart Grid Communications, 2011 IEEE International Conf. on. IEEE, 2011, pp. 505–510.

[16] A. Khodaei, "Microgrid optimal scheduling with multi-period islanding constraints," Power Systems, IEEE Transactions on, vol. 29, no. 3, pp. 1383–1392, 2014.

[17] A. J. Wood and B. F. Wollenberg, Power generation, operation, and control. John Wiley & Sons, 2012.

[18] K. Morison, P. Kundur, and L. Wang, "Critical issues for successful on-line security assessment," Real-Time Stability in Power Systems: Techniques for Early Detection of the Risk of Blackout, p. 147, 2005.

[19] R. L.-Y. Chen and C. A. Phillips, "k-edge failure resilient network design," Electronic Notes in Discrete Mathematics, vol. 41, pp. 375–382, 2013.

[20] B. Stott, O. Alsac, and A. J. Monticelli, "Security analysis and optimization," Proceedings of the IEEE, vol. 75, no. 12, pp. 1623–1644, 1987.

[21] H. Nagarajan, E. Yamangil, R. Bent, P. Van Hentenryck, and S. Backhaus, "Optimal resilient transmission grid design," in Power Systems Computation Conference (PSCC), 2016. IEEE, 2016, pp. 1–7.

[22] M. Mohanpurkar and S. Suryanarayanan, "Accommodating unscheduled flows in electric grids using the analytical ridge regression," IEEE Transactions on Power Systems, vol. 28, no. 3, pp. 3507–3508, 2013.

[23] Y. Hayashi and J. Matsuki, "Loss minimum configuration of distribution system considering n-1 security of dispersed generators," IEEE Transactions on power systems, vol. 19, no. 1, pp. 636–642, 2004.

[24] S. Mashayekh, M. Stadler, G. Cardoso, M. Heleno, S. Chalil Madathil, H. Nagarajan, R. Bent, M. Mueller-Stoffels, X. Lu, and J. Wang, "Security-constrained design of isolated multi-energy microgrids," 2017, under review at IEEE transactions on Power Systems.

[25] A. Bischi, L. Taccari, E. Martelli, E. Amaldi, G. Manzolini, P. Silva, S. Campanari, and E. Macchi, "A detailed milp optimization model for combined cooling, heat and power system operation planning," Energy, vol. 74, pp. 12–26, 2014.

[26] S. Bahramirad, W. Reder, and A. Khodaei, "Reliability-constrained optimal sizing of energy storage system in a microgrid," IEEE Transactions on Smart Grid, vol. 3, no. 4, pp. 2056–2062, 2012.

[27] O. Hafez and K. Bhattacharya, "Optimal planning and design of a renewable energy based supply system for microgrids," Renewable Energy, vol. 45, pp. 7–15, 2012.

[28] S. Bahramara, M. P. Moghaddam, and M. Haghifam, "Optimal planning of hybrid renewable energy systems using homer: A review," Renewable and Sustainable Energy Reviews, vol. 62, pp. 609–620, 2016.

[29] Z. Bie, P. Zhang, G. Li, B. Hua, M. Meehan, and X. Wang, "Reliability evaluation of active distribution systems including microgrids," IEEE Transactions on Power Systems, vol. 27, no. 4, pp. 2342–2350, 2012.

[30] M. E. Baran and F. F. Wu, "Network reconfiguration in distribution systems for loss reduction and load balancing," Power Delivery, IEEE Transactions on, vol. 4, no. 2, pp. 1401–1407, 1989.

[31] I. Koutsopoulos, V. Hatzi, and L. Tassiulas, "Optimal energy storage control policies for the smart power grid," in Smart Grid Communications, 2011 IEEE International Conf. on. IEEE, 2011, pp. 475–480.

[32] "Caterpillar generator data," Caterpillar, 2 2016, 41205 /40476 /41431 /8427. [Online]. Available: http://s7d2.scene7.com/is/content/Caterpillar/LEHE0489-00

[33] J. W. Kolar, T. Friedli, F. Krismer, A. Looser, M. Schweizer, R. A. Friedemann, P. K. Steimer, and J. B. Bevirt, "Conceptualization and multiobjective optimization of the electric system of an airborne wind turbine," IEEE Journal of Emerging and Selected Topics in Power Electronics, vol. 1, no. 2, pp. 73–103, 2013.

[34] A. Czanderna, G. Jorgensen, C. E. Witt, M. Al-Jassim, and J. M. Gee, "Service lifetime prediction for encapsulated photovoltaic cells/minimodules," in AIP Conference Proceedings, vol. 394, no. 1. AIP, 1997, pp. 295–312.

[35] "Abb central inverters pvi-500.0-cn 500 kw," ABB, 5 2014, rev. A EN. [Online]. Available: https://goo.gl/k8lv2C
[36] "Nps 100c-24 brochure – north america," Northern Power Systems. [Online]. Available: https://goo.gl/wu8Dz7
[37] I. Dunning, J. Huchette, and M. Lubin, "Jump: A modeling language for mathematical optimization," SIAM Review, vol. 59, no. 2, pp. 295–320, 2017.
[38] W. H. Kersting, "Radial distribution test feeders," in Power Engineering Society Winter Meeting, 2001. IEEE, vol. 2. IEEE, 2001, pp. 908–912.
[39] K. Sundar, H. Nagarajan, M. Lubin, L. Roald, S. Misra, R. Bent, and D. Bienstock, "Unit commitment with n-1 security and wind uncertainty," in Proceedings of the 19th Power Systems Computation Conference, 2016.
[40] E. Yamangil, R. Bent, and S. Backhaus, "Resilient upgrade of electrical distribution grids." in AAAI, 2015, pp. 1233–1240.

Sreenath Chalil Madathil is a doctoral candidate from Department of Industrial Engineering at Clemson University, Clemson, SC. He received the MS in Industrial Engineering from Clemson University in 2013 and B.Tech from Federal Institute of Science and Technology, India in 2006. His research interest include operations research, simulation, energy systems and security analysis.

Emre Yamangil received his PhD in Operations Research from Rutgers University under the supervision of Professor Endre Boros. His research focuses on various aspects of mixed-integer convex or non-convex optimization. He joined Los Alamos National Laboratories as a post-doctoral associate after his PhD. During this time he worked on designing reliable distribution and transmission power grids. Currently he is studying applications of deep learning on computational photography and computer vision at Snap Inc. as a software engineer.

Harsha Nagarajan received the Ph.D. degree in Mechanical Engineering from Texas A&M University, College Station, in 2014, in the area of Controls and Optimization. Currently, he is a scientist at "Applied Mathematics and Plasma Physics" division at the Los Alamos National Laboratory, Los Alamos, NM, USA. His research interests include solving a myriad of problems in the fields of control theory and (discrete/non-convex) optimization applied to energy infrastructure systems and UAV routing.

Arthur Barnes (S'03) received the B.Sc. degree in electrical engineering from the University of Colorado, Boulder, CO, USA, in 2003, and the M.Sc. in electrical engineering degree from the University of Florida, Gainesville, FL, USA, in 2007. He received his Doctorate degree in electrical engineering at the University of Arkansas, Fayetteville, AR, USA in 2014. He is currently at Los Alamos National Laboratory, where he his studying resilience of the electric power grid.

Russell Bent A-1, Los Alamos National Laboratory, Los Alamos, United States. Russell Bent received the Ph.D. degree in computer science from Brown University, Providence, RI, USA. He has been a scientist at Los Alamos National Laboratory (LANL), Los Alamos, NM, USA, since 2005, in the Information Systems and Modeling group. At LANL, he leads a team of researchers focused on developing next-generation algorithms for planning, operating, and designing critical infrastructure systems. He is the principal or co-principal investigator for numerous DOE, DHS, and DOD projects in these areas, with focuses on improving robustness of power systems, increasing resilience of distribution networks, modeling interdependencies between systems, managing disasters that impact critical infrastructure, modeling smart grid technologies, and developing methods for stochastic optimization. He is the author of one book, Online Stochastic Combinatorial Optimization, and over 60 peer reviewed journal and conference publications (see http://public.lanl.gov/rbent/). Dr. Bent is an associate editor for the INFORMS Journal of Computing.

Scott Backhaus received the Ph.D. degree in physics from the University of California at Berkeley, Berkeley, CA, USA, in 1997, in the area of macroscopic quantum behavior of superfluid He-3 and He-4. He is currently the Principal Investigator for several LANL projects funded by the Office of Electricity in the U.S. Department of Energy, is an LANL Program Manager for Office of Electricity and for DHS Critical Infrastructure, and leads LANL's component of the DHS National Infrastructure Simulation and Analysis Group.

Scott J. Mason is the Fluor Endowed Chair in Supply Chain Optimization and Logistics and a Professor of Industrial Engineering at Clemson University. He received his Ph.D. in Industrial Engineering from Arizona State University after earning Bachelor's and Master's degrees from The University of Texas at Austin. Dr. Mason's research focuses on developing optimization-based solutions for planning, scheduling, and controlling large-scale supply chain systems. His email address is mason@clemson.edu.

Salman Mashayekh received the B.S. and M.S. degrees in electrical power systems from University of Tehran, Iran, in 2006 and 2008, respectively, and the Ph.D. degree from Texas A&M University, College Station, TX, USA, in 2013. Currently, he is a scientist at Lawrence Berkeley National Lab, Berkeley, CA, USA. His research interests are in power and energy management methods in microgrids and buildings, electrical and cyber security in smartgrids, and applications of optimization in power and energy systems.

Michael Stadler is a Staff Scientist at Lawrence Berkeley National Laboratory. He leads the Grid Integration Group and the Microgrid team at Berkeley Lab. He is a recipient of the Presidential Early Career Award for Scientists and Engineers (PECASE) Award of the White House. He studied at Vienna University of Technology, from which he holds a Master's degree in electrical engineering and a Ph.D. summa cum laude in energy economics. He advises the Department of Defense on microgrid design and multi-level microgrid controllers based on IEEE 2030.7.